

STATUS OF THE SHORT-PULSE SOURCE AT DELTA*

A. Held[†], A. Radha Krishnan, B. Büsing, H. Kaiser, S. Khan, D. Krieg, C. Mai
Center for Synchrotron Radiation (DELTA), Dortmund, Germany

Abstract

At the synchrotron light source DELTA operated by the TU Dortmund University, the short-pulse facility employs the seeding scheme coherent harmonic generation (CHG) and provides ultrashort pulses in the vacuum ultraviolet and terahertz regime. Here, the interaction of laser pulses with the stored electron bunches results in a modulation of the longitudinal electron density which gives rise to coherent emission at harmonics of the laser wavelength. Recently, investigations of the influence of the Gouy phase shift at the focal point of the laser pulses on the laser-electron interaction have been performed. For the planned upgrade towards echo-enabled harmonic generation (EEHG) with a twofold laser-electron interaction, simulations of the ideal parameters of the laser beams have been carried out.

THE DELTA SHORT-PULSE SOURCE

At the university-based electron storage ring DELTA, the short-pulse source employs the seeding scheme coherent harmonic generation (CHG) [1]. As depicted in Fig. 1 (top), CHG is based on a laser-electron interaction in an undulator (modulator). This results in a sinusoidal modulation of the electron energy, which is transformed into a density modulation (microbunches) via a magnetic chicane. In a subsequent undulator (radiator), the microbunch structure leads to coherent emission at harmonics of the laser wavelength with a pulse duration similar to that of the laser pulse. At DELTA, the magnetic setup is realized in a single undulator with three individually powered sections to act as modulator, chicane and radiator. Ultrashort pulses from a 1-kHz 8-mJ Ti:sapphire laser system at wavelengths of 800-nm or 400-nm laser pulses are used for the seeding process.

In a planned upgrade, the more sophisticated seeding scheme echo-enabled harmonic generation (EEHG) [2] will be implemented. It requires another laser-electron interaction and a strong chicane prior to the magnetic setup used for CHG (see Fig. 1 bottom). Here, the final density profile consists of microbunches with a high-frequency substructure enabling coherent radiation at much higher harmonics compared to CHG. In 2017, tests implementing a two-fold laser-electron interaction were successfully carried out. Here, a phase-stable interaction of the electrons with laser pulses at 800 nm and 400 nm was achieved [3]. The new magnetic lattice in the EEHG section was finalized while the optics elsewhere will remain the same. Two new undulators to be used as modulators as well as their respective girders and vacuum chambers have been delivered.

* Work supported by the BMBF (05K16PEA, 05K16PEB, 05K19PEC), MERCUR (Pr-2014-0047), DFG (INST 212/236-1 FUGG) and the state of NRW.

[†] arne.held@tu-dortmund.de

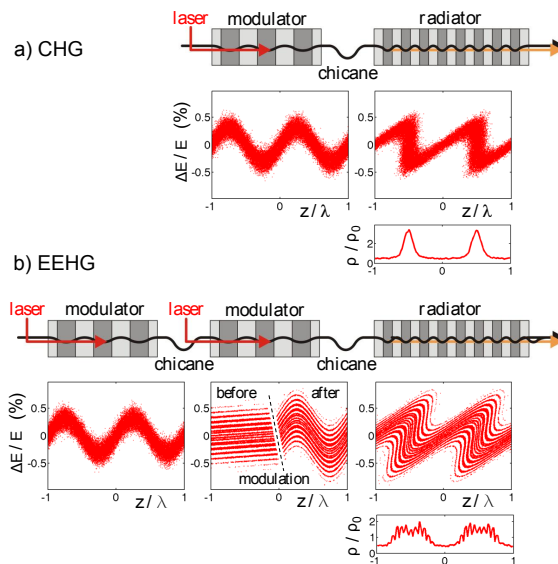


Figure 1: Magnetic setup for a) CHG and b) EEHG with corresponding longitudinal phase space distributions and final longitudinal electron density.

LASER-ELECTRON INTERACTION AND GOUY PHASE SHIFT

A relativistic electron in an undulator interacts with a co-propagating laser field. Modeling its field as a plane wave, the undulator needs to be tuned to the laser wavelength to modulate the electron energy. A more realistic scenario is a Gaussian laser beam with its focal point at the undulator center. This introduces the Gouy phase shift, an additional phase advance depending on the distance to the laser focal point. As a result, the laser phase velocity exceeds the speed of light c near the focal point affecting the wavelength the undulator needs to be tuned to.

The on-axis electric field \vec{E}_L of a Gaussian laser beam with wavelength λ_L is given by

$$|\vec{E}_L(t)| = E_0 \frac{w_0}{w(z)} \cos \left(k_L z - \omega_L t - \arctan \left(\frac{z}{z_R} \right) + \phi_0 \right),$$

with the focal size w_0 , the Rayleigh length $z_R = \pi w_0^2 / \lambda_L$, the beam size $w(z) = w_0 \sqrt{1 + (z/z_R)^2}$, the amplitude of the electric field at the focus E_0 , the Gouy phase shift $-\arctan(z/z_R)$ and a phase offset ϕ_0 . The energy transfer then results [4] in

$$dW = -\frac{ecE_0K}{2\gamma} \frac{w_0}{w(z)} (\sin \Psi_+ - \sin \Psi_-) dt.$$

Summed over all undulator periods, a net energy change requires the phase,

$$\Psi_+ = (k_L + k_U)z - \omega_L - \arctan \left(\frac{z}{z_R} \right) + \phi_0,$$

to be constant in time while Ψ_- may oscillate. If the Rayleigh length exceeds the undulator length, the approximation $\arctan(z/z_R) \approx z/z_R$ can be applied. With the average velocity along an undulator

$$\dot{z} = 1 - \frac{1}{2\gamma^2} \left(1 + \frac{K^2}{2} \right) c,$$

the optimum of the fundamental undulator wavelength λ_{fund} is given by the condition

$$\frac{d\Psi_+}{dt} \stackrel{!}{=} 0 = \left(k_L + k_U - \frac{1}{z_R} \right) \dot{z} - \omega_L$$

$$\Leftrightarrow \lambda_{\text{fund}} = \frac{\lambda_U}{2\gamma^2} \left(1 + \frac{K^2}{2} \right) = \left(1 - \frac{\lambda_U}{2\pi z_R} \right) \lambda_L.$$

Thus, the undulator must be tuned to a wavelength smaller than λ_L for a laser beam focussed at the undulator center with $\lambda_L = \lambda_{\text{fund}}$ for a plane wave with $z_R \rightarrow \infty$.

In an experiment at DELTA, the undulator parameter K of the modulator with $\lambda_U = 25$ cm and total length 1.75 m was varied while monitoring a laser-induced THz signal. Moving the laser focus longitudinally by about 2 m drastically reduces the total Gouy phase advance along the undulator, such that its effect on the matching condition is reduced. As shown in Fig. 2, the optimum undulator wavelength λ_{fund} is indeed closer to the laser wavelength around 800 nm when the laser focus is shifted away from the undulator center.

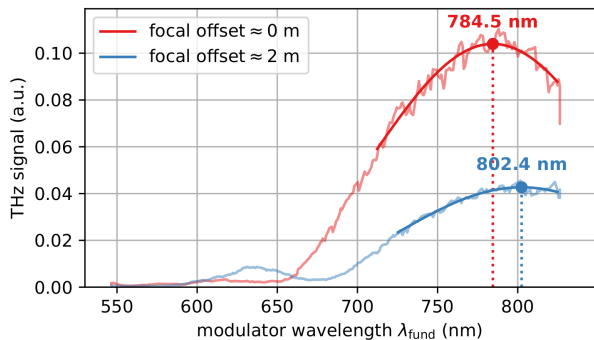


Figure 2: Laser-induced THz signal under variation of the fundamental modulator wavelength with the 800-nm laser beam focus centered at the modulator (red) and shifted by 2 m (blue).

SIMULATION OF TWO-FOLD LASER-ELECTRON INTERACTION

In the planned EEHG setup, two individual laser-electron interactions are required for which the straight section will be modified with two new undulators. Using the already existing Ti:sapphire laser system, EEHG seeding is possible at a wavelength of 800 nm, 400 nm or 266 nm radiation using second- or third-harmonic generation (SHG, THG).

In all simulations, the laser wavelength λ_1 for the first energy modulation was chosen to be 800 nm. To estimate the

optimal laser parameters and to compare different choices of λ_2 , simulations of laser-electron interaction in the two modulators were carried out using *ELEGANT* [5] with the undulator and laser parameters listed in Table 1. The chicane strengths $R_{56}^{(1,2)}$ were optimized for a maximum bunching factor at the 41st harmonic of 800 nm.

Table 1: Parameters used for Simulations

Laser parameters	SHG	THG
Wavelength	800 nm	400 nm 266 nm
Pulse energy	2 mJ	1 mJ 0.35 mJ
Pulse length (FWHM)		40 fs
Quality factor M^2		2.0
Undulator period length	20 cm (7 periods)	

In one trial, the bunching factor was calculated for different laser waist sizes $w_0^{(1)}$ of the first laser while keeping the waist size $w_0^{(2)}$ of the second laser fixed (Fig. 3, top). For all three cases, the bunching factor initially increases with $w_0^{(1)}$, reaches a maximum at around 1.4 mm and decreases for larger $w_0^{(1)}$. The initial increase can be attributed to the improved homogeneity of the energy modulation as the laser waist size increases. Furthermore, the bunching factor is known to have a positive correlation with the amplitude of first energy modulation ΔE_1 [6] which explains the decrease for larger $w_0^{(1)}$.

In another run, $w_0^{(1)}$ was fixed at 1.4 mm and $w_0^{(2)}$ was varied (Fig. 3, bottom). In this case, the bunching factor increases initially with $w_0^{(2)}$ and remains constant for larger waist sizes. Compared to $w_0^{(1)}$, the influence of $w_0^{(2)}$ on the bunching factor is much larger because the second energy modulation is applied to the striated phase space distribution after the first chicane. This demands the second energy modulation to be very uniform in order not to smear out the fine density pattern.

For large waist sizes, the energy modulation amplitude will be too small to be converted to a corresponding density modulation for given maximum chicane strength. The dotted vertical lines in Fig. 3 represent this limit for each choice of modulating wavelength assuming $R_{56}^{(1)} = 1.5$ mm for the first chicane.

Results for the 41st harmonic of 800 nm suggest that both wavelengths, 400 nm and 266 nm, used for the second energy modulation result in a similar bunching factor of around 0.1. In the 266-nm case, one could achieve a larger bunching factor if the maximum strength of the first chicane was larger which, however, is limited by the space available in the straight section.

DESIGN OF THE CHICANES

Electromagnetic simulations of the chicanes were carried out using *CST-Microwave Studio* [7]. The chicane parameters are listed in Table 2. The second chicane follows a standard 4-magnet design, while the first chicane employs

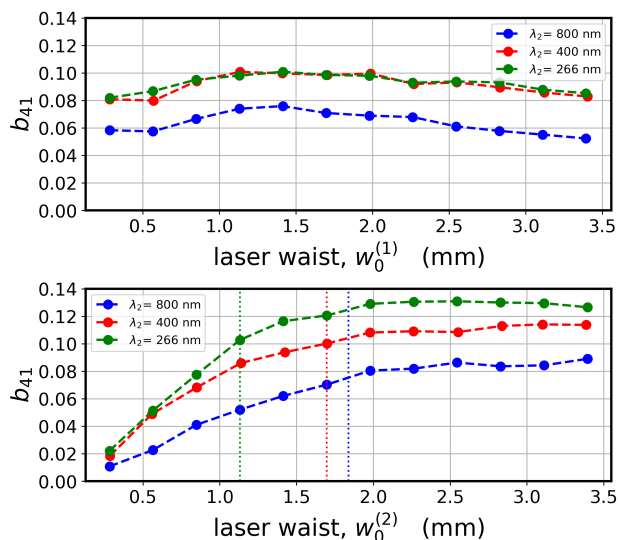


Figure 3: Bunching factor at the 41st harmonic of 800 nm for different laser waist sizes and modulating wavelengths. The first modulating laser wavelength is 800 nm for all three cases. The vertical dotted lines (bottom plot) represent the maximum waist size for each choice of λ_2 .

5 magnets of alternating polarities to keep the maximum horizontal displacement of the electrons sufficiently small so that the present vacuum chamber can be used.

Table 2: Chicane Parameters

	1st Chicane	2nd Chicane
Total length	1.92 m	0.75 m
No. of magnets	5	4
Max. current	500 A	400 A
Max. R_{56}	1.73 mm	0.2 mm
Max. hor. deflection	11.15 mm	5.38 mm
Additional path length	0.868 mm	0.1 mm

The transfer matrix elements R_{51} and R_{52} of the chicanes couple the longitudinal displacement to the horizontal position x_0 and divergence x'_0 of a particle. For a perfect chicane, both should be zero to avoid position- and angle-dependent distortions of the density modulations. However, field errors and imperfections in the magnets would result in non-zero values of R_{51} and R_{52} . As can be seen in Fig. 4, this effect is much more deleterious in the second chicane. Considering an electron beam size of 0.5 mm at the location of the second chicane, the $R_{51}^{(2)}$ must be in the order of 10^{-6} to achieve sufficient microbunching at wavelengths around 20 nm. Extra care must be given to manufacturing magnets with extremely good field quality and in their implementation. In addition, the use of corrector coils is foreseen.

CONCLUSION

At the DELTA short-pulse source, laser-induced energy modulation to generate ultra-short pulses via CHG is rou-

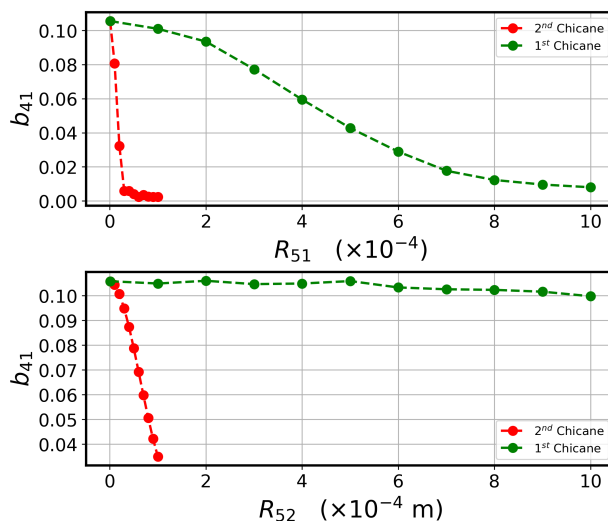


Figure 4: Effect of non-zero R_{51} (top) and R_{52} (bottom) on the bunching factor of the 41st harmonic of 800 nm.

tinely performed. Recently, the influence of the Gouy phase shift of laser pulses on the laser-electron interaction could be verified. With the laser beam focused at the center of the modulator, its fundamental wavelength must be tuned to be significantly smaller than the laser wavelength.

Implementation of the EEHG scheme is planned as an upgrade. Simulations show that both options for the second seed pulse, $\lambda_2 = 400$ nm or 266 nm, can be optimized for a maximum bunching factor of 0.1 at 19.5 nm. Further studies related to the output quality of the SHG/THG units are required for a more realistic estimate of the bunching factor before finalizing the decision.

A preliminary design of the magnetic chicanes was carried out. Simulations reveal that even moderate values of R_{51} and R_{52} of the chicanes can destroy microbunches.

ACKNOWLEDGEMENTS

We are pleased to thank our colleagues at DELTA and the TU Dortmund University. The continuous support from other institutes, particularly from DESY Hamburg, HZB Berlin, and KIT Karlsruhe is gratefully acknowledged.

REFERENCES

- [1] R. Coisson and F. De Martini, “Free-electron coherent relativistic scatterer for UV-generation”, *Quantum Electronics*, vol. 9, p. 939, 1982.
- [2] G. Stupakov, “Using the beam echo effect for generation of short-wavelength radiation”, *Phys. Rev. Lett.*, vol. 102, p. 074801, 2009. doi:10.1103/PhysRevLett.102.074801
- [3] S. Khan *et al.*, “Seeding of electron bunches in storage rings”, in *Proc. 38th Int. Free Electron Laser Conf. (FEL17)*, Santa Fe, NM, USA, Aug. 2017, pp. 94–97. doi:10.18429/JACoW-FEL2017-MOP027

- [4] P. Schmüser, M. Dohlus, J. Rossbach, and C. Behrens, *Free-electron Lasers in the ultraviolet and X-ray regime*, Switzerland: Springer Int. Publishing, 2014.
- [5] M. Borland, "ELEGANT: A flexible SDDS-compliant code for accelerator simulation", ANL, Argonne, IL, USA, Rep. LS-287, 2000.
- [6] D. Xiang and G. Stupakov, "Echo-enabled harmonic generation free electron laser", *Phys. Rev. Spec. Top. - Accel. Beams*, vol. 12, p. 030702, 2009.
doi:10.1103/PhysRevSTAB.12.030702
- [7] CST STUDIO SUITE ®, <https://www.cst.com/products/csts2>